available at www.sciencedirect.com
ScienceDirect
journal homepage: www.elsevier.com/locate/agwat
Agricultural Water Management

Evaluation of urea–ammonium–nitrate fertigation with drip irrigation using numerical modeling

Blaine R. Hanson [a], *Jirka Šimůnek* [b], *Jan W. Hopmans* [a,*]

[a] *LAWR, University of California, 123 Veihmeyer Hall, Davis, CA 95616, United States*
[b] *Environmental Sciences, University of California, Riverside, CA, United States*

ARTICLE INFO

Article history:
Accepted 12 June 2006
Published on line 30 August 2006

Keywords:
Irrigation
Nitrogen management
Microirrigation
Nitrate leaching

ABSTRACT

Microirrigation with fertigation provides an effective and cost-efficient way to supply water and nutrients to crops. However, less-than-optimum management of microirrigation systems may cause inefficient water and nutrient use, thereby diminishing expected yield benefits and contributing to ground water pollution if water and nitrogen applications are excessive. The quality of soils, ground, and surface waters is specifically vulnerable in climatic regions where agricultural production occurs mostly by irrigation such as in California. Robust guidelines for managing microirrigation systems are needed so that the principles of sustainable agriculture are satisfied. The main objective of this research was to use an adapted version of the HYDRUS-2D computer model to develop irrigation and fertigation management tools that maximize production, yet minimize adverse environmental effects. This software package can simulate the transient two-dimensional or axisymmetrical three-dimensional movement of water and nutrients in soils. In addition, the model allows for specification of root water and nitrate uptake, affecting the spatial distribution of water and nitrate availability between irrigation cycles. Recently, we analyzed four different microirrigation systems in combination with five different fertigation strategies for various soil types using a nitrate-only fertilizer, clearly demonstrating the effect of fertigation strategy on the nitrate distribution in the soil profile and on nitrate leaching. In the present study, the HYDRUS-2D model was used to model the distribution of soil nitrogen and nitrate leaching using a urea–ammonium–nitrate fertilizer, commonly used for fertigation under drip irrigation. In addition, the distribution of phosphorus and potassium was modeled. Model simulations are presented for surface drip and subsurface drip tape, each associated with a typical crop in California.

1. Introduction

Microirrigation with fertigation provides an effective and cost-efficient way to supply water and nutrients to crops (Bar-Yosef, 1999). However, less-than-optimum management of microirrigation systems resulting in excessive water and nitrogen applications may result in inefficient water and nutrient use, thereby diminishing expected yield benefits and contributing to ground water pollution. The quality of soils, ground, and surface waters is specifically vulnerable in climatic regions where agricultural production occurs mostly by irrigation, such as in California. Liquid nitrogen (N) fertigation, using mixtures of urea, ammonium, and nitrate compounds, is widely used with microirrigation. Robust guidelines for managing microirrigation systems are needed so that the principles of sustainable agriculture are satisfied.

* *Corresponding author*. Tel.: +1 530 752 3060; fax: +1 530 752 5262.
E-mail addresses: brhanson@ucdavis.edu (B.R. Hanson), Jiri.Simunek@ucr.edu (J. Šimůnek), jwhopmans@ucdavis.edu (J.W. Hopmans).

doi:10.1016/j.agwat.2006.06.013

The mathematical formulation with corresponding analytical solutions of transient transport in soils to include transformation of ammonia and nitrate for steady state water flow was presented by Misra et al. (1974). Wagenet et al. (1977) extended the theory to include urea transport, determining the control of soil oxygen concentration, and initial urea concentration on urea hydrolysis. The various N transformation processes in soils occur mostly by microbial processes that are predicted by first-order reaction kinetics, but are complex because of their coupled nature and their control by soil environmental conditions such as soil water and temperature. Nitrogen transport and transformations with transient water flow to include plant uptake, nitrification, denitrification, immobilization, mineralization, and ionic exchange was modeled for the first time by Selim and Iskandar (1981) by simultaneously solving the transport equations for the different N species with the purpose to evaluate nitrogen fate for a wide range of nitrification rate, ammonium retardation and N-uptake values. Other one-dimensional models, that were specifically developed for N-transport in soils, include the simulation model by Tanji et al. (1981), DAISY (Hansen et al., 1990), LEACHN (Hutson and Wagenet, 1991), COUP (Jansson and Karlberg, 2001), and the lumped parameter model LPM (Ling and El-Kadi, 1998).

While high field-scale uniformity is possible under microirrigation, the distribution of both water and nitrate about the drip line is very nonuniform. Both soil water content and chemical concentration will be the highest near the drip line after application, but water and chemicals will redistribute thereafter as controlled by soil physical properties. Because of the typical nonuniform wetting patterns, it is essential to use multi-dimensional modeling to develop optimal fertigation practices for optimum nutrient use efficiency. In the absence of experimental data, we can use mathematical solutions of the governing multi-dimensional water and nutrient transport equations to evaluate the multi-dimensional aspects of nitrate fertigation. Yet, few computer simulation models have the capability to analyze water flow and nutrient transport in multiple spatial dimensions, with the exception of HYDRUS-2D (Somma et al., 1998; Šimůnek et al., 1999; Cote et al., 2003) and FUSSIM2 (Heinen, 2001). The HYDRUS model allows for specification of root water and nitrate uptake, affecting the spatial distribution of water and nitrate availability between irrigation cycles. As documented by Weinbaum et al. (1992) and later by Hopmans and Bristow (2002), few studies evaluated the interrelationships between rates and spatial distribution of N application, root distribution and growth, and total plant uptake. Most recently, a first step in this general direction was achieved by Gärdenäs et al. (2005), where four different microirrigation systems were analyzed in combination with five different fertigation strategies for various soil types, clearly demonstrating the effects of root distribution and fertigation strategy on the uniformity of water and nutrients around drip lines and their effects on water drainage and associated nitrate leaching.

In concept, the rhizosphere dynamics of water and nutrient uptake is very complex, and may have to consider differentiation between passive and active nutrient uptake, while including N mineralization (Bar-Yosef, 1999), denitrification and rhizosphere acidity (Pierre and Banwart, 1973). In order to not be overcome by these many complications of which the relative magnitude and relevance is yet to be determined, this study makes the typical assumption that root uptake of ammonium and nitrate is strictly passive and assumes that the other listed mechanisms are not occurring.

The main objective of this study was to use a state-of-the-art modeling tool to evaluate irrigation and fertigation practices. For that purpose we applied the HYDRUS-2D model (Šimůnek et al., 1999) to evaluate the control of fertigation strategy with microirrigation on both the movement and fate of a liquid urea–ammonium–nitrate fertilizer, mixed with phosphorus and potassium in the irrigation water for two commonly used microirrigation systems.

2. Materials and methods

The modeling of water flow and fertigation scenarios was conducted using an adapted version of the computer simulation model HYDRUS-2D (Šimůnek et al., 1999). This software package can simulate the transient two-dimensional or axisymmetrical three-dimensional movement of water and nutrients in soils. In addition, the model allows for specification of root water and nitrate uptake, affecting the spatial distribution of water and nitrate availability between irrigation cycles. The database of the model contains the values of the parameters specifying the hydraulic properties for the various soil types that are required for the simulation model. For each soil type and emitter type, the spatial patterns of water content and nitrate concentration were determined for various fertigation strategies. These strategies included different nutrient injection durations, different injection times relative to the irrigation set time, and different concentrations. Model simulations will be presented for two different pressurized irrigation systems, each associated with a typical crop and representing two commonly used microirrigation systems in California: surface drip (DRIP; grape) and subsurface drip tape (SUBTAPE; processing tomatoes).

2.1. *Modeling domain and nitrogen reactions*

The irrigation layouts for the two selected microirrigation systems with characteristic dimensions, including emitter and irrigation line spacing, are presented in Fig. 1, whereas relevant irrigation application and model parameters are presented in Table 1. DRIP (Fig. 1A) is considered a point source so that axisymmetric-radial geometry is assumed, whereas the SUBTAPE (Fig. 1B) layout was simulated using the line-source model with a rectangular geometry, because of the multiple outlets along the tape. The model domain for these microirrigation system layouts represents the area explored by roots, based on field measurements and experience (Bassoi et al., 2003; May and Hanson, 2005). More detailed information about the simulation model and model parameters can be found in Gärdenäs et al. (2005).

Irrigation water concentrations of phosphorus and potassium were 1.0 M L^{-3}, while applied irrigation water concentrations for urea, ammonium, and nitrate were 0.5, 0.25, and 0.25 M L^{-3}, respectively, with nitrogen concentrations corresponding to the proportion of nitrogen in the fertilizer solution

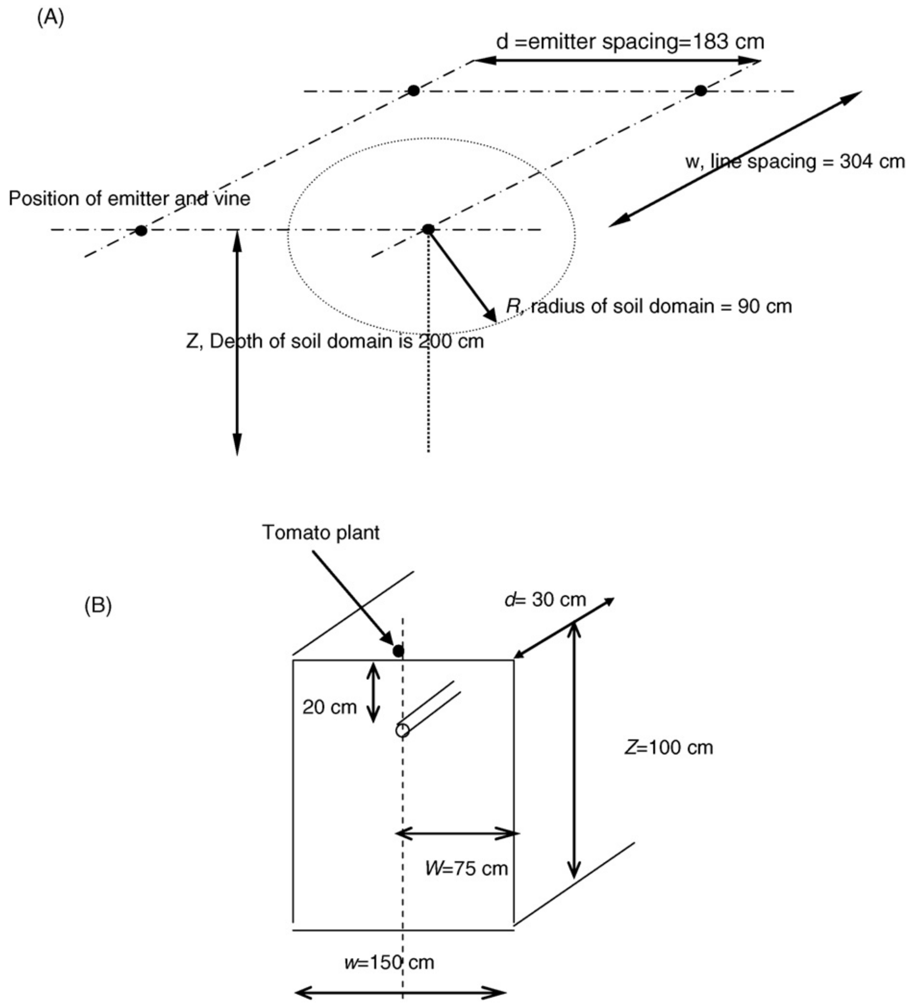

Fig. 1 – Simulation domains for: DRIP (A) and SUBTAPE (B).

consisting of 16.5% urea nitrogen, 7.4% ammonium nitrogen, and 7.4% nitrate nitrogen. These input concentrations expressed in $M L^{-3}$ allows for general use of the model. Specifically, input concentrations can be multiplied with field-applied amounts at equal proportions, so that simulated and experimental results can be compared. Using these proportional concentrations, it should be clear that the total nitrate concentration in the soil solution can never be higher than $1.0 M L^{-3}$, irrespective of transformations between N species.

HYDRUS-2D allows simultaneous simulation of multiple solutes that can be either independent of each other (P and/or K) or subject to the first-order degradation reactions (nitrogen species). The first-order decay chain of urea is described as follows (Tillotson et al., 1980):

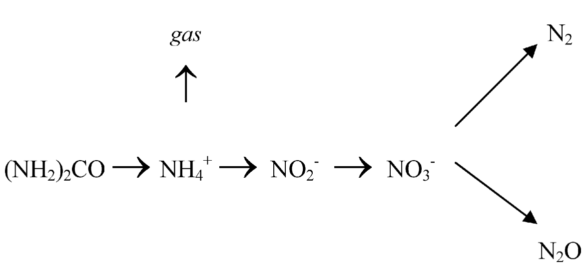

In this reaction pathway urea is hydrolyzed by heterotrophic bacteria to form ammonium, which is sequentially nitrified by autotrophic bacteria to nitrite and nitrate, that is subsequently denitrified to form di-nitrogen (N_2 and N_2O). Ammonium is a volatile species that can also be present in the gas phase (*gas*). Since the nitrification from nitrite to nitrate is a much faster reaction than nitrification of ammonium, both nitrification reactions are often lumped, thereby neglecting the nitrite species.

2.2. *Coupled water flow and solute transport equations*

The spatial distributions of transient water content and volumetric flux were obtained using a numerical solution of the Richards equation:

$$\frac{\partial\theta(h)}{\partial t} = \frac{\partial}{\partial x_i}\left[\left(K_{ij}(h)\frac{\partial h}{\partial x_j} + K_{iz}(h)\right)\right] - S(h) \quad (1)$$

where θ is the volumetric water content $[L^3 L^{-3}]$, h the pressure head [L], S the sink term $[L^3 L^{-3} T^{-1}]$, representing root water uptake as a function of spatial position and time, x_i (i = 1, 2) the spatial coordinates [L], t the time [T], and K_{ij} are components of

Table 1 – Irrigation system characteristics

	DRIP (grape)	SUBTAPE (tomatoes)
Irrigation		
Discharge rate, Q_0 (L day^{-1})	90.72	11.975
Irrigation intensity, q_o (cm day^{-1})	1.63	2.66
Irrigation duration, P (days)	1.5	1.15
Irrigation interval, ΔP (days)	3.5	3.5
Emitter (d) and line (w) spacing (cm)	183 × 304	30 × 150
Depth of emitter (cm)	0	20
Water demand:		
ET_0 (cm day^{-1})	0.7	0.7
Crop coefficient, K_c	0.85	1.06
Simulated domain		
Width, W (cm)	n.a.	75
Radius, R (cm)	90	n.a.
Depth, Z (cm)	200	100
Root water uptake		
The critical water pressure heads in Feddes model h_1, h_2, h_{3max}, h_{3min}, h_4 (cm)	−1, −2, −1000, −1000, −8000	−1, −2, −800, −1500, −8000
Root zone		
Root distribution model	Vrugt model	Vrugt model
Maximum rooting depth, z_m (cm)	90	100
Depth with max root density, z^* (cm)	0	20
Maximum lateral root extension, r_m (cm)	90	75
Distance r with max root density, r^* (cm)	0	0
Non-symmetry coefficients, p_z and p_r	1.0,1.0	1.0,1.0

n.a., not applicable.

the hydraulic conductivity tensor $\mathbf{K}$ [L T^{-1}] defined as the product of the relative hydraulic conductivity, $K_r(h)$, and the saturated hydraulic conductivity tensor, $\mathbf{K}_s$ [L T^{-1}]. Since in our simulations we assume that the porous medium is isotropic, the saturated hydraulic conductivity tensor has the off-diagonal entries equal to 0 and the diagonal terms equal to the saturated hydraulic conductivity, K_s [L T^{-1}]. The Richards equation was solved using HYDRUS-2D that provides numerical solutions for both two-dimensional (SUBTAPE) and axi-symmetrical three-dimensional (DRIP) problems (Gärdenäs et al., 2005).

The partial differential equations governing two-dimensional nonequilibrium chemical transport of solutes involved in a sequential first-order decay chain during transient water flow in a variably saturated rigid porous medium are:

$$\frac{\partial \theta c_1}{\partial t} + \rho \frac{\partial s_1}{\partial t} = \frac{\partial}{\partial x_i}\left(\theta D_{ij,1}\frac{\partial c_1}{\partial x_j}\right) - \frac{\partial q_i c_1}{\partial x_i} - \mu_{w,1}\theta c_1 - \mu_{s,1}\rho s_1 - Sc_{r,1} \quad (2)$$

$$\frac{\partial \theta c_k}{\partial t} + \rho \frac{\partial s_k}{\partial t} = \frac{\partial}{\partial x_i}\left(\theta D_{ij,k}\frac{\partial c_k}{\partial x_j}\right) - \frac{\partial q_i c_k}{\partial x_i} - \mu_{w,1}\theta c_k - \mu_{s,k}\rho s_k + \mu_{w,k-1}\theta c_{k-1} + \mu_{s,k-1}\rho s_{k-1} - Sc_{r,k}, \quad k\,\varepsilon\,(2, n_s) \quad (3)$$

where c and s are solute concentrations in the liquid [M L^{-3}] and solid [M M^{-1}] phases, respectively; q_i the ith component of the volumetric flux density [L T^{-1}], μ_w and μ_s first-order rate constants for solutes in the liquid and solid phases [T^{-1}], respectively, providing connections between individual chain species, ρ the soil bulk density [M L^{-3}], S the sink term [L^3 L^{-3} T^{-1}] in the water flow equation (Eq. (1)), c_r the concentration of the sink term [M L^{-3}], D_{ij} the dispersion coefficient tensor [L^2 T^{-1}] for the liquid phase, subscript k the kth chain number, and n_s is the number of solutes involved in the chain reaction. The last term in both equations represents passive nutrient uptake through the product of root water uptake, S, and species concentration.

The adsorption isotherm relating s_k and c_k is described by a linear equation of the form

$$s_k = K_{d,k} c_k \quad (4)$$

where $K_{d,k}$ [L^3 M^{-1}] is the distribution coefficient of species k.

Eq. (2) represents either the first species in the chain reaction (urea) or an independent species (P and K), while Eq. (3) represents second and other solutes in the sequential first-order decay chain (ammonium and nitrate). Note that the first-order decay coefficient μ acts as sink in Eq. (2) and as a source in Eq. (3). Relative concentrations can be used since all transport and reaction parameters (K_d, μ) are concentration independent and thus both transport equations are linear.

2.3. *Parameter values and boundary conditions*

2.3.1. Parameter values

Urea (Eq. (2)), ammonium and nitrate (Eq. (3)) were considered for the nitrogen species simulations. While urea and nitrate were assumed to be present only in the dissolved phase (i.e., K_d = 0 cm^3 g^{-1}), ammonium was assumed to adsorb to the solid phase using a *distribution coefficient* K_d of 3.5 cm^3 g^{-1}. Similar values were reported in the literature: K_d = 3–4 cm^3 g^{-1} by Lotse et al. (1992), K_d = 1.5 cm^3 g^{-1} by Selim and Iskandar (1992), and K_d = 3.5 cm^3 g^{-1} by Ling and El-Kadi (1998). The first-order decay coefficient μ_w for urea, representing *hydrolysis*, was set to be

0.38 day^{-1}. Again, similar values were used in the literature, for example by Ling and El-Kadi (1998) who considered hydrolysis to be in the range of 0.36, 0.38, and 0.56 day^{-1}. *Nitrification* from ammonium to nitrate was modeled using the rate coefficient of 0.2 day^{-1}, which represents the center of the range of values reported in the literature, e.g., 0.2 day^{-1} by Jansson and Karlberg (2001), 0.02–0.5 day^{-1} by Lotse et al. (1992), 0.226–0.432 day^{-1} by Selim and Iskandar (1992), 0.15–0.25 day^{-1} by Ling and El-Kadi (1998), and 0.24–0.72 day^{-1} by Misra et al. (1974). Volatilization of ammonium and subsequent ammonium transport by gaseous diffusion was neglected.

Although HYDRUS-2D allows for denitrification, the presented simulations did not account for any denitrification to occur. Although we included denitrification initially, results were unsatisfactory because of the large sensitivity of denitirification rates on the model results; yet little information on denitrification rate as a function of the soil moisture regime under drip irrigation is available. Therefore, denitrification was not considered at this time.

There is also relatively large uncertainty concerning the values of the distribution coefficients for phosphorus and potassium. In our simulations we used values derived from Silberbush and Barber (1983), i.e., $K_d = 59.3\ cm^3\ g^{-1}$ for phosphorus and 28.7 $cm^3\ g^{-1}$ for potassium. For phosphorus, this is in the range of 19 $cm^3\ g^{-1}$ reported by Kadlec and Knight (1996) and of 185 $cm^3\ g^{-1}$ reported by Grosse et al. (1999). We assumed that the bulk density was equal to 1.5 $g\ cm^{-3}$, the longitudinal dispersivity was equal to 5 cm, with the transverse dispersivity being one-tenth of the longitudinal dispersivity, and neglected molecular diffusion as it was considered negligible relative to dispersion.

2.3.2. Initial and boundary conditions

Each of the fertigation scenarios was preceded by 56 days of flow-only simulations, to approach a 'pseudo-equilibrium' condition before irrigation with fertigation started. This was done to ensure that the initial soil water regime was not a factor in the transport and leaching predictions (Gärdenäs et al., 2005). The initial condition for this initialization period was set to a uniform soil water pressure head of −400 cm. The soil hydraulic parameters of the van Genuchten (1980) model for the loam were taken from Carsel and Parrish (1988). The transport domain was considered to be solute free at the beginning of the fertigation simulation.

All boundaries were assumed to be no flow boundaries with the exception of the bottom of the soil profile and the boundary representing the irrigation device. A unit gradient boundary condition for water flow and the Neumann boundary condition for solute transport were used at the bottom of the soil profile. System dependent boundary conditions representing irrigation devices were described in detail by Gärdenäs et al. (2005) and are listed in Table 1. The selected parameters for the Feddes et al. (1978) water stress response function were taken from van Dam et al. (1997), and are presented in Table 1 as well. Root distribution in the soil profile was assumed to be described using Vrugt's model (Vrugt et al., 2001). The values of the root distribution parameters in Table 1 reflect typical root systems for the two irrigated cropping systems and were introduced by Gärdenäs et al. (2005) to represent maximum rooting depths of about 100 cm.

2.3.3. Irrigation system parameters

The irrigation requirement, Q_{req} (L day^{-1}), was computed from the crop-specific potential evapotranspiration (ET_c) (cm day^{-1}) and the irrigated soil area, $A = dw$, where d (cm) and w (cm) represent emitter distance and irrigation line distance, respectively. Selected ET_c values are typical values for California irrigated crops. The model also included an evaporation component for the DRIP simulations (Gärdenäs et al., 2005). The applied irrigation volume per irrigation cycle, I [cm^3], was estimated for each crop from Q_{req}, the irrigation interval, ΔP [days], and the irrigation efficiency, f_i. For all irrigation systems, we assumed an irrigation efficiency of 85% (Hanson, 1995). Thus, plant water uptake was less than the applied water for all scenarios. Finally, the irrigation cycle duration, P (day^{-1}), was determined from the total irrigation volume, I, and the emitter discharge rate, Q_o. Specific values for each of the two studied microirrigation systems are presented in Table 1.

2.4. Fertigation scenarios

Similar to the study of Gärdenäs et al. (2005), we considered three fertigation strategies to evaluate water and nutrient use efficiency and nitrate leaching. These are based on recommendations of the microirrigation industry and grower's practices. These are (B) fertigation for a total duration of 2 h, starting 1 h after the beginning of the irrigation cycle; (E) fertigation for a duration of 2 h, starting 3 h before the end of the irrigation cycle; and (M50), starting the first and last 25% of each irrigation with fresh water, and fertigation during the remaining 50% in the middle of the irrigation cycle. The fresh water irrigations prior and after each fertigation are common practices that ensure uniformity of fertilizer application and flushing of the drip lines. Each irrigation cycle was simulated for 28 days and included eight irrigation cycles with fertigation. The irrigation cycle length (P) and other crop-specific irrigation characteristics are presented in Table 1.

3. Results and discussion

The effects of different fertigation strategies on the soil distribution of urea, ammonium, and nitrate around a drip line between the first and second irrigation and at the end of the simulation period are illustrated in Figs. 2–6. The effect of the B strategy is discussed in detail for the DRIP system for the total simulation period of 28 days, while only presenting the main results of the other strategies. Time $t = 0$ is the start of the fertigation simulation after the 56 days of flow-only simulations. All fertilizer concentrations are expressed as nominal concentrations, relative to the concentration of the fertilizer in the irrigation water. The same mass of fertilizer was applied for each fertigation strategy.

3.1. Distributions around drip line

3.1.1. Soil water content

Soil water content at the start of DRIP irrigation was relatively low near the soil surface (Fig. 2). The water content was

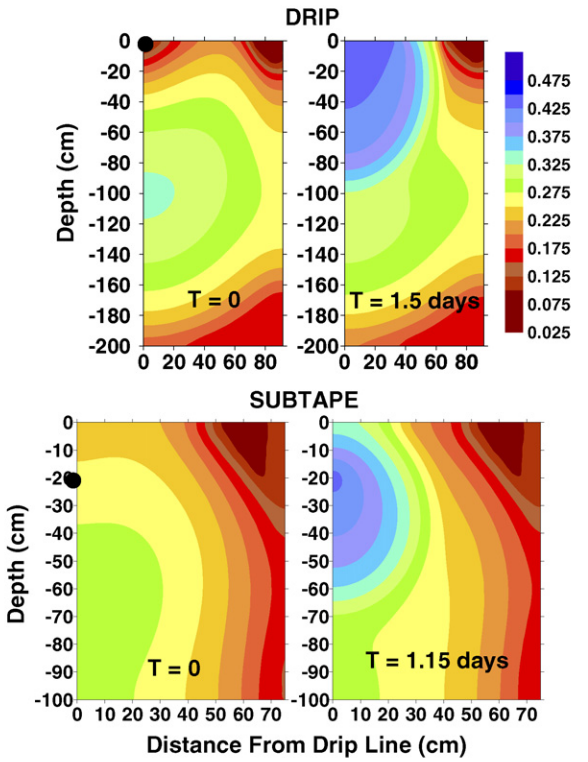

Fig. 2 – Volumetric soil water content distributions at the start and conclusion of irrigation for DRIP and SUBTAPE microirrigation systems.

maximum between the 60 and 140 cm soil depth, and was controlled by root water uptake. After each irrigation, the wetted region exhibited a vertically elongated pattern and extended to nearly 60 cm horizontally and 100 cm vertically directly beneath the emitter. A zone of relatively wet soil occurred near the surface between 40 and 60 cm from the drip line. This distinct wetting front position is the combined result of wetting front advance during irrigation and a decreased root distribution density away from the drip line.

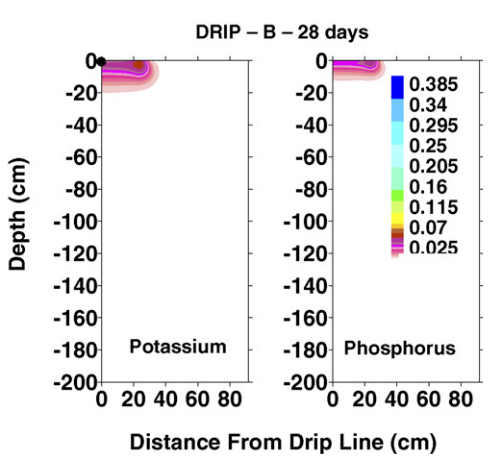

Fig. 3 – Spatial distributions of potassium and phosphorus concentration (M L^{-3}) in soil solution at the end of the simulation period (28 days) for the B strategy of DRIP.

Before irrigation with the SUBTAPE system, water content values were smallest near the surface, decreasing with horizontal distance from the drip line (Fig. 2). The soil was slightly wetter at depths below about 35 cm. After irrigation, most wetting occurred above the 70 cm soil depth and extending to near the soil surface. Horizontal water movement was limited to about 35 cm from the drip line. Soil water contents beyond 35 cm at the end of the irrigation were the same as those at the start of irrigation.

3.1.2. DRIP—B

The contour plots in Figs. 3–6 show the simulated concentrations of nutrients in the soil water. Both potassium and phosphorus were present only immediately adjacent to the drip line at all times (Fig. 3), independent of irrigation type or fertigation scenario. This was the case at all times, as both fertilizers are highly adsorbed by the soil, preventing their movement further down the soil profile. It should be pointed out at this time that the model simulations only considered matrix flow, thus excluding the possibility of rapid transport of nutrients by preferential flow. The B fertigation strategy generally resulted in a band of urea along the periphery of the wetted soil volume (Fig. 4) with little or no urea near the drip line, except immediately after fertigation ($t = 3.63$). There was relatively little change during subsequent irrigation cycles, indicating that little urea accumulation occurred in the soil profile. However, urea concentrations decreased with time between irrigations as a result of hydrolysis. As expected, at 3.63 days, the urea was concentrated near the drip line, immediately after fertigation. Some slight preferential lateral movement occurred, likely because of occasional soil surface ponding and larger horizontal water potential gradients.

As for K and P, ammonium remained concentrated in the immediate vicinity of the drip line at all times for all fertigation strategies (Fig. 4). There was only slight movement, because of soil adsorption and subsequent fast nitrification and/or root uptake.

In contrast to ammonium, nitrate moved continuously downwards during the 28-day simulation period, as nitrate is not adsorbed, whereas denitrification was assumed negligible. As expected, high nitrate concentrations occurred near the drip line immediately after fertigation ($t = 3.63$) due to nitrate injection and nitrification, but little nitrate remained near the drip line at the end of the irrigation ($t = 5.00$, Fig. 4), because of root uptake and dispersion during downward transport. At this time, most of the nitrate was distributed near the periphery of the wetted region due to leaching following the fertigation. However, by the start of the next irrigation ($t = 7.00$), nitrate levels near the drip line increased, the result of nitrification of ammonium. The relatively high concentration of nitrate near the drip line at $t = 7.00$ reflected the distribution of ammonium. Between irrigations, nitrate concentrations near the drip line decreased with time due to redistribution and root water uptake. In general, except for times immediately after fertigation, nitrate concentrations were relatively low, with the highest values along the wetting front. Bands of nitrate reflect the wetting patterns after each irrigation cycle. At the end of the last irrigation event of the simulation period, nitrate was distributed throughout the

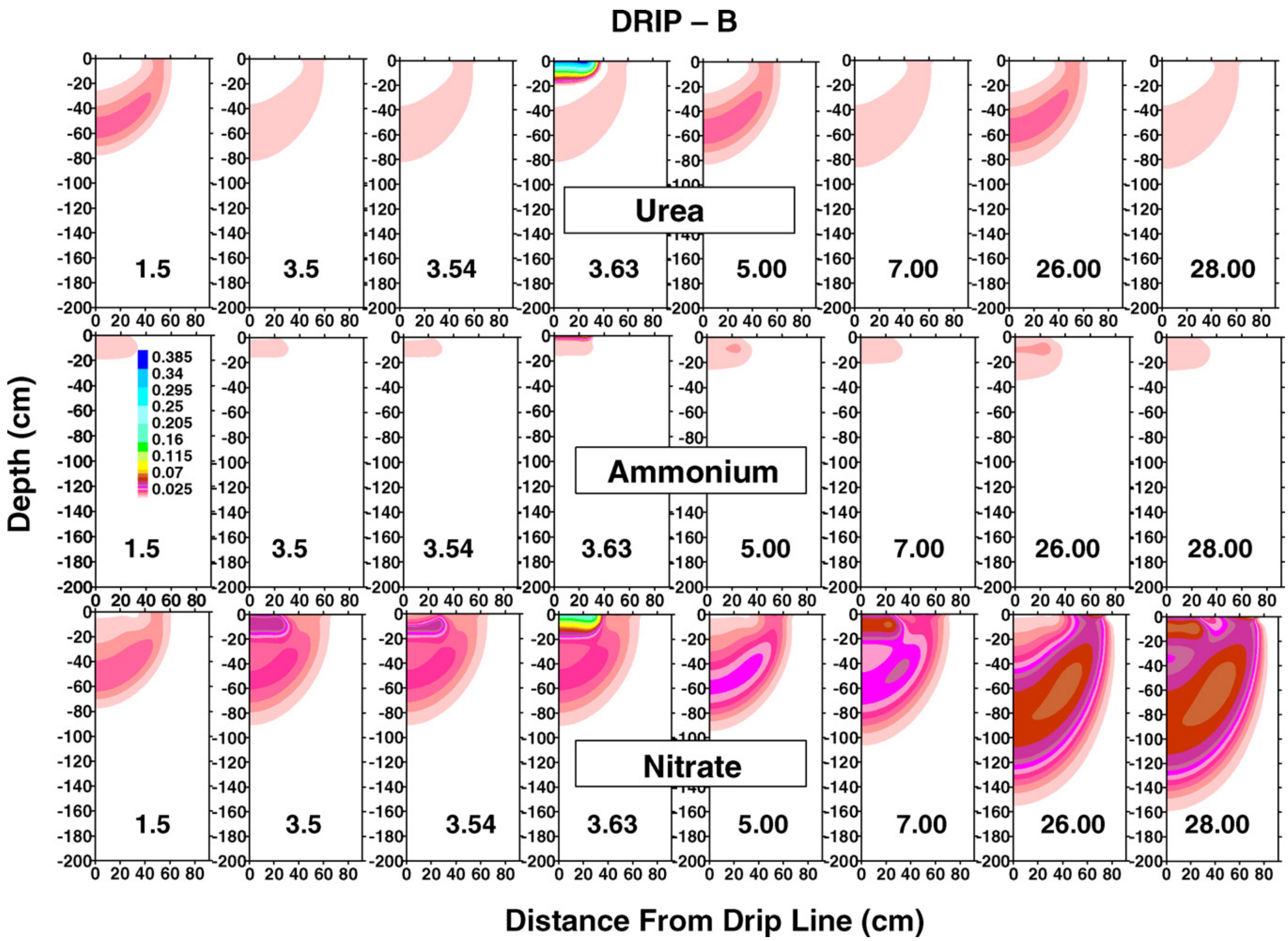

Fig. 4 – Spatial distributions of soil solution urea, ammonium, and nitrate ($M L^{-3}$) for the B strategy of DRIP for various days during the simulation period. The times (days) correspond to end of first irrigation (1.50), beginning of the second irrigation (3.5), beginning of second fertigation (3.54), end of second fertigation (3.63), end of second irrigation (5.00), beginning of third irrigation (7.00), end of last irrigation (26.00), and end of simulation period (28.00).

wetted soil profile to a soil depth of about 150 cm, indicating potential leaching after 28 days.

3.1.3. DRIP—E

In the case of fertigation at the end of the irrigation cycle (Fig. 5), urea concentrations were maximum near the drip line with concentrations decreasing with time between irrigation cycles as a result of hydrolysis and water redistribution. A noticeable second front occurred at a larger depth because of water movement by irrigation prior to the start of fertigation ($t = 4.88$). As before, ammonia concentrations remained high near the drip line. Nitrate was concentrated near the edge of the wetted region due to irrigation before fertigation (Fig. 5). After fertigation ($t = 4.96$), nitrate was maximum near the drip line, but then decreased slightly by the end of the irrigation ($t = 5.00$). As with the B strategy, nitrate concentrations increased near the drip line due to ammonium nitrification by the start of the next irrigation ($t = 7.00$). At the end of the last irrigation event of the simulation period, nitrate was distributed throughout the wetted soil profile to a soil depth of about 150 cm, similar to that of the B strategy. However, nitrate concentrations throughout the profile were smaller than those of the B strategy except near the drip line, where higher concentrations occurred for the E strategy compared to the B strategy.

3.1.4. DRIP—M50

Fertigation during the middle 50% of the irrigation event caused a more uniform and more extended urea distribution throughout the wetted region compared to the other fertigation strategies (Fig. 5), because of larger fertigation times. Henceforth, maximum urea concentrations near the drip line were lower than for the B and E scenarios. Because of its adsorption, ammonium distributions around the drip line were similar to those of the other scenarios. As with urea, nitrate was distributed more uniformly throughout the wetted region as compared to the other scenarios (Fig. 5). After fertigation (4.63 days), nitrate concentrations throughout the profile increased with time, particularly near the drip line as shown for the distribution at 7.00 days. Because of hydrolysis and nitrification, nitrate accumulated in the soil profile with time, extending vertically to about 150 cm below the drip line and 80 cm horizontally by the end of the simulation period.

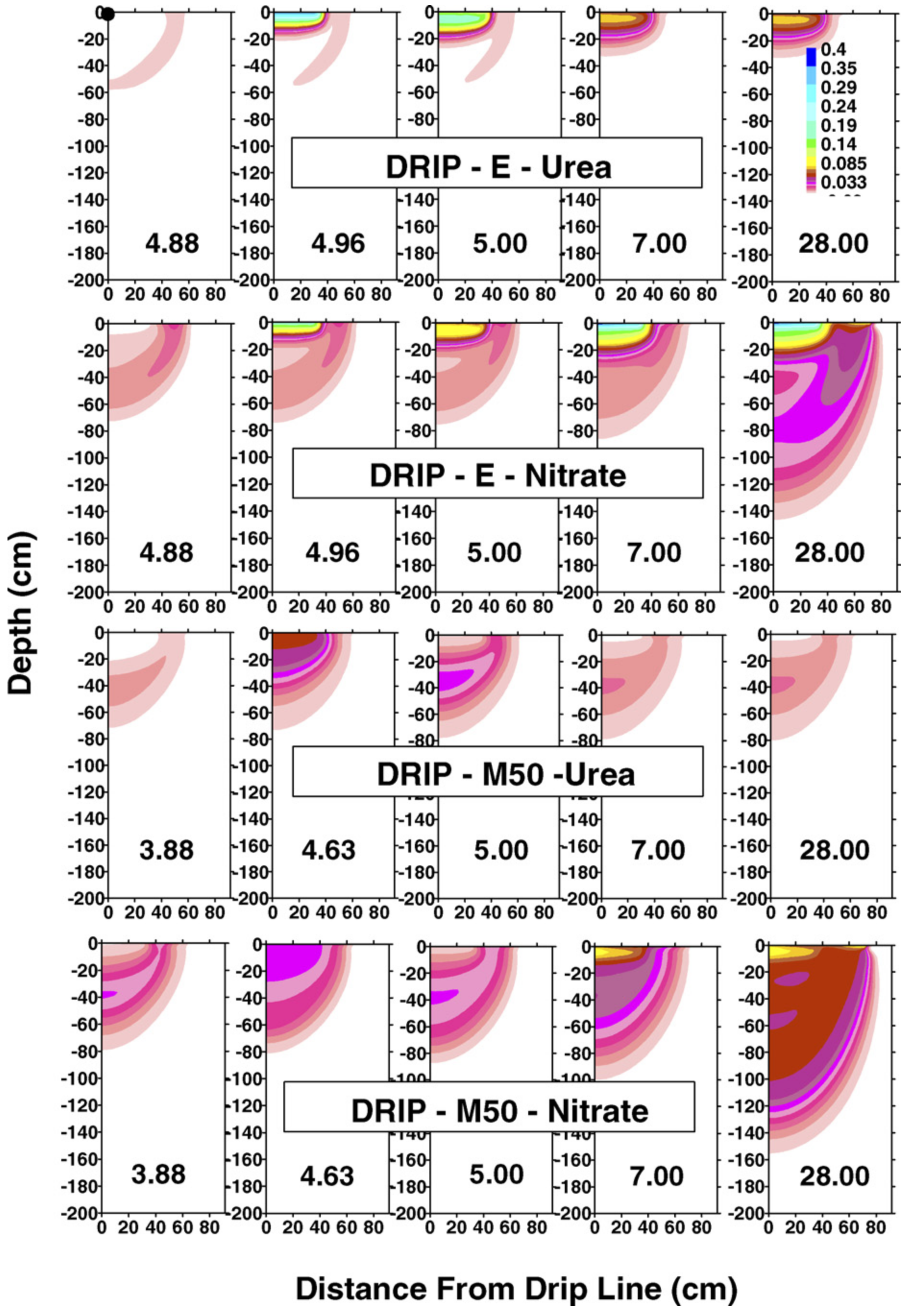

Fig. 5 – Spatial distributions of soil solution urea and nitrate (M L^{-3}) for selected times of the E and M50 strategies of DRIP. For the E strategy, the times (days) correspond to the beginning of second fertigation (4.88), end of second fertigation (4.96), end of second irrigation (5.00), beginning of next irrigation (7.00), and end of simulation period (28.00). For the M50 strategy, the times (days) correspond to the same sequence of events as described for the E strategy.

3.1.5. *SUBTAPE—B, E, and M50*

The various species distributions for urea and nitrate for the three fertigation scenarios are presented in Fig. 6. Overall, results are comparable with the DRIP irrigation system, except that spatial distribution patterns are controlled by the buried irrigation drip line, thereby carrying ammonia and nitrate to larger depths. As expected, phosphorus and potassium remained close to the drip line (results not shown). For the B strategy, urea and nitrate were moved away from the drip line during irrigation, whereas both species remained near the drip line for the E strategy. After irrigation at $t = 4.65$ days, nitrate concentrations near the drip line increased due to nitrification. Whereas urea concentrations decreased between irrigation cycles as a result of hydrolysis, nitrate concentrations accumulated with time throughout the soil profile during the 28-day irrigation period. Between irrigation events the nitrate concentrations decreased because of root uptake.

The nitrate concentrations below the drip line for the B scenario were lower than those above the drip line due to capillary upward movement during irrigation, which was the

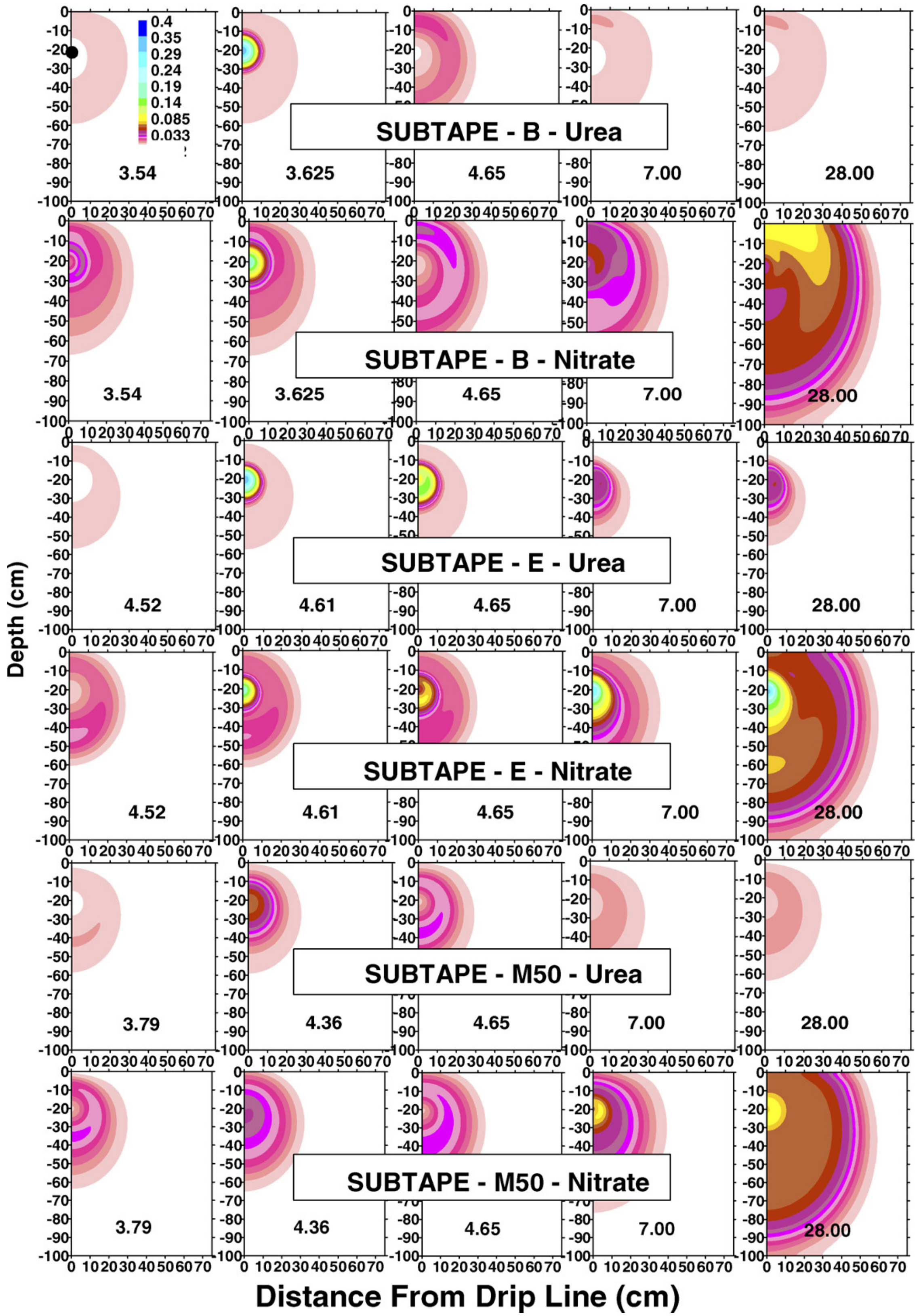

Fig. 6 – Spatial distribution of urea and nitrate ($M L^{-3}$) for selected times for the B, E, and M50 strategies for SUBTAPE. The respective times correspond to the beginning of the second fertigation, end of the second fertigation, end of the second irrigation, beginning of the next irrigation, and end of the simulation period for each fertigation strategy.

opposite for the E strategy. For the M50 strategy, nitrate was distributed more uniformly throughout the wetted region as compared to the B and E strategies (Fig. 6).

3.2. *Mass balance*

Since we used dimensional concentrations in our simulations, the dimension of mass in the mass balance calculations are either [M] for the axi-symmetric geometry of DRIP or [M cm^{-1}] for the two-dimensional geometry of SUBTAPE, and includes the sorbed mass.

3.2.1. *DRIP*

The mass balance was conducted for two zones, the upper 100 cm or root zone (zone 1) and the lower 100 cm (zone 2). It was assumed that the accumulated nitrate in zone 2 eventually will leach out of the simulated soil domain, because of the absence of roots in zone 2. As expected, the urea mass was maximal at the end of the each fertigation event, but decreased with time thereafter until the next fertigation event (Fig. 7), because of subsequent hydrolysis. The mass values of the first fertigation event reflect mass ratios of the applied fertilizer mixture. No accumulation of urea occurred in the profile and no urea moved to zone 2 as all urea either converted to ammonium by hydrolysis. The urea mass was similar for all fertigation strategies. Ammonium accumulation was limited to zone 1, and no ammonia was present in zone 2 because of the relatively quick nitrification and slow transport due to sorption.

We computed a slight increase in ammonium between irrigation events, indicating that its supply from fertilizer and urea hydrolysis exceeded removal by plant uptake and nitrification. Typically, the mass of ammonium increased between the end of the fertigation and the end of the irrigation during which that fertigation event occurred, due to hydrolysis. In contrast, nitrate accumulated with time for all fertigation strategies indicating that supply of nitrate by the fertilizer and nitrification of ammonium exceeded removal by plant uptake and leaching. Because of the transport of nitrate by the infiltrating irrigation water, nitrate also accumulated in zone 2 during the second half of the simulation period.

The N mass balance at 28 days is shown in Table 2. More N root uptake occurred for the E strategy compared to the B and M50 strategies. The accumulated N pertains to zone 1 only, as it was assumed that all nitrate in zone 2 (below rooting zone) will potentially leach. Leached N (below zone 1) was the

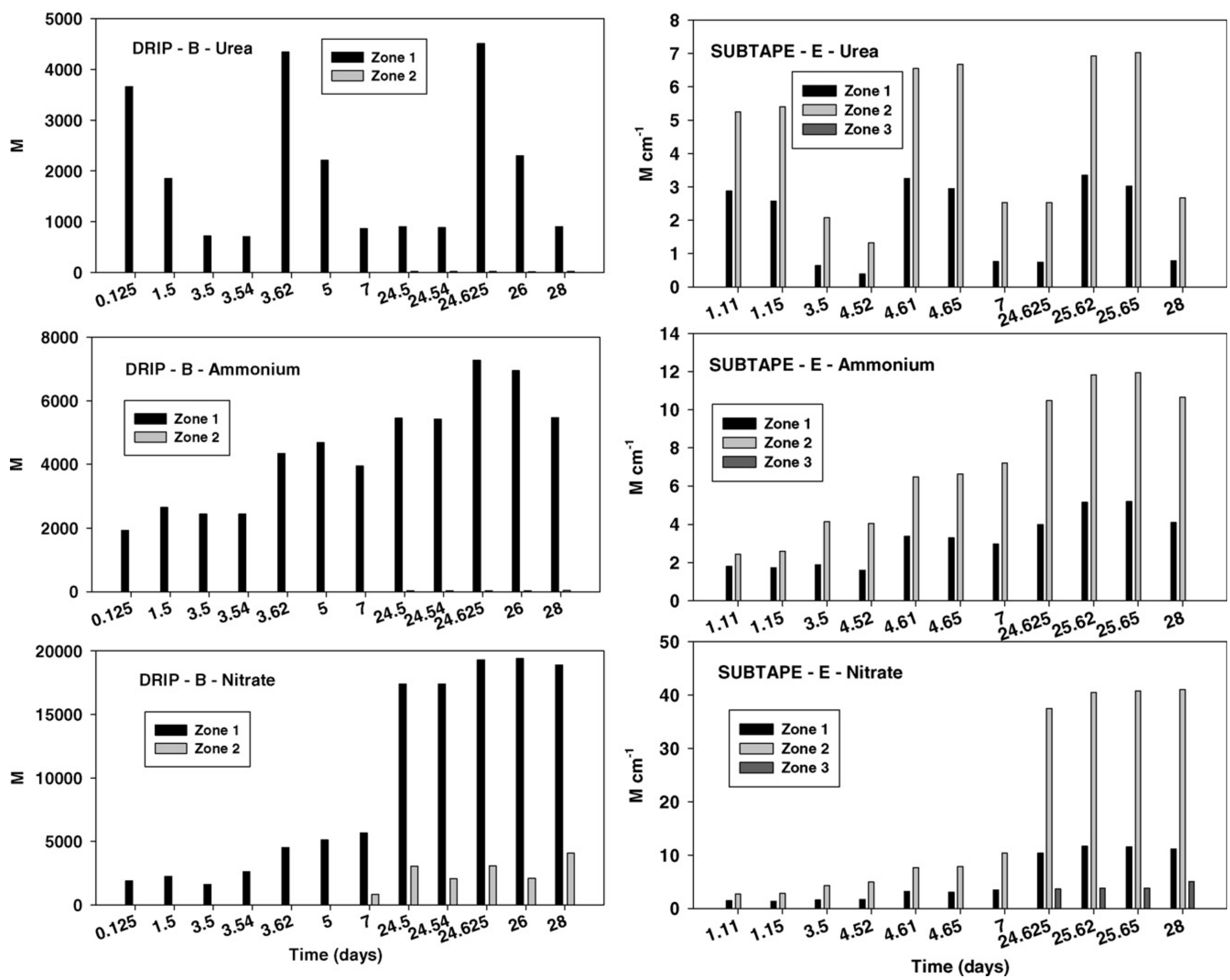

Fig. 7 – Total mass (M) of urea, ammonium, and nitrate with time during the simulation period for the B strategy of DRIP and for the E strategy of SUBTAPE.

Table 2 – Nitrogen mass balance for DRIP and SUBTAPE microirrigation systems and B (fertigation near beginning of irrigation), E (fertigation near the end of irrigation), and M50 (fertigation during the middle 50% of the irrigation event) fertigation strategies

	B	E	M50
DRIP			
Input (M)	60400	60400	60400
Root uptake (M)	30600	39185	33052
Accumulated (M)	25272	20090	24690
Leached (M)	4120	1560	3139
Leached (%)	6.8	2.6	5.2
FUE (%)	50.7	64.9	54.7
SUBTAPE			
Input (M cm^{-1})	133	133	133
Root uptake (M cm^{-1})	59.7	58.6	57.3
Accumulated (M cm^{-1})	68.4	70.4	70.4
Leached (M cm^{-1})	5.1	5.1	5.7
Leached (%)	3.9	4.0	4.4
FUE (%)	46.6	45.8	44.8

FUE is the fertilizer use efficiency. M denotes mass of nitrogen.

smallest for the E strategy. The mass balance showed leaching percentages of 6.8, 2.6, and 5.2% for the B, E, and M50 fertigation strategies, respectively. These leaching percentages were slightly lower than those found using a nitrate-only fertilizer (Gärdenäs et al., 2005). As expected, no leaching of ammonium or urea took place.

The fertilizer use efficiency (FUE), calculated as the ratio of the mass of N uptake to the mass applied, ranged from 50.7 to 64.9% (Table 2). The E scenario showed the highest efficiency and the B strategy was the lowest.

3.2.2. *SUBTAPE*

For the SUBTAPE irrigation system, the soil profile was split into three zones: zone 1 above the drip line, zone 2 below the drip line to the 75 cm soil depth, and zone 3 the bottom 25 cm of the soil profile. It was assumed that the accumulated nitrate in zone 3 would eventually leach out of the simulated soil domain because of the lack of roots in zone 3. The urea mass decreased with time following fertigation, however, more urea was found in zone 2 compared to zone 1 (Fig. 7), because of the location of the subsurface tape. No urea was present in zone 3. Both ammonium and nitrate mass accumulated during the simulation period, with more mass in zone 2 than in zone 1. This behavior occurred for all fertigation strategies. No ammonium was present in zone 3. Nitrate leached into zone 3 near the end of the simulation period. Urea, ammonium, and nitrate masses were higher in zone 1 and lower in zone 2 for the B strategy as compared to the E and M50 strategies. This result reflects the increased opportunity for upward flow of water and dissolved N species by capillarity near the beginning of irrigation of the B scenarios.

The results of the mass balance at 28 days (Table 2) indicated similar N uptake for all fertigation strategies. Accumulated and leached masses were also similar for all strategies. Leaching percentages were 3.9, 3.9, and 4.4% for the B, E, and M50 fertigation strategies, respectively. FUE's were nearly equal between strategies (44.8–46.6%), with slight differences caused by upward movement above the drip line.

4. Conclusions

We conclude that the HYDRUS-2D computer simulation model is an effective modeling tool for assessing fertigation strategies using a urea–ammonium–nitrate fertilizer commonly used for fertigation with microirrigation. The model described the movement of urea, ammonium, and nitrate during irrigation and accounted for the reactions of hydrolysis, nitrification, and ammonium adsorption.

In contrast to the previous study (Gärdenäs et al., 2005) which used a nitrate-only fertilizer, the model showed that a urea–ammonium–nitrate fertilizer increased the nitrate concentration near the drip line, an area where root density is greatest and most of the plant root uptake of nitrate takes place. This was also the case for the B strategy with a long irrigation after fertigation. Nitrification of ammonium maintained nitrate concentrations near the drip line compared to the nitrate-only fertilizer, in part caused by the sorption of ammonium prior to nitrification, thereby delaying downward transport of soil nitrate.

The results also showed that urea moves readily with the infiltrating irrigation water, potentially moving this nitrate source away from the soil zone with maximum root density. For all strategies, urea did not accumulate in the soil profile, but quickly decreased with time after fertigation by hydrolysis and associated conversion to ammonium. Because of its adsorption to the soil, most of the ammonium remained near the drip line, with low concentrations near the edge of the wetting zone.

Nitrate mass accumulated in the soil profile, moving down to depths deeper than 150 cm for the DRIP system and deeper than 100 cm for SUBTAPE. Higher nitrate mass occurred above the drip line for the B strategy compared to the other strategies for SUBTAPE. The leached nitrate mass was smallest for the E fertigation strategy and largest for the B strategy for the DRIP system. No trends were clearly determined for any fertigation strategy for the SUBTAPE irrigation system, mainly due to upward flow and associated movement of N species above the drip line.

Slightly smaller leaching percentages were computed for the urea–ammonium–nitrate fertilizer compared to the nitrate-only fertilizer. Fertilizer use efficiency ranged from 50.7% (B strategy) to 64.9% (E strategy) for DRIP and was about 44–47% for SUBTAPE. Based on these results we conclude that fertigations consisting of short injection times near the beginning of long irrigation events should be avoided for surface drip systems. The fertigation strategy is less of a factor for subsurface drip systems.

For the presented irrigation scenarios the position of the drip lines coincided with the plant rows. Thus, the input root distributions reflect typical wetting patterns as determined from field data, with maximum soil water content and root density near the drip lines and decreasing with distance and depth from the drip line. For other scenarios where drip lines are placed away from the plant rows, we expect different spatial distributions of roots and soil water content, as roots will adapt to changing soil water regimes. An additional limitation of our model results comes about from the absence of denitrification. The disregard of denitrification was intentional as there is no information available on denitrification rates for soil moisture regimes under micro-irrigation. Nevertheless, our simulation results provide guidance on the appropriate fertigation strategy for many typical microirrigation scenarios.

Acknowledgement

We acknowledge funding by the California FREP, Fertilizer Research and Education Program.

REFERENCES

Bar-Yosef, B., 1999. Advances in fertigation. Adv. Agron. 65, 1–75.

Bassoi, L.H., Hopmans, J.W., de, L.A., Jorge, C., De Alencar, C.M., Silva, J.A.M.E., 2003. Grapevine root distribution in drip and microsprinkler irrigation using monolith and the soil profile method. Scientia Agricola 60 (2), 377–387.

Carsel, R.F., Parrish, R.S., 1988. Developing joint probability distributions of soil water retention characteristics. Water Resour. Res. 24, 755–769.

Cote, C.M., Bristow, K.L., Charlesworth, P.B., Cook, F.J., Thorburn, P.J., 2003. Analysis of soil wetting and solute transport in subsurface trickle irrigation. Irrig. Sci. 22, 143–156.

Feddes, R.A., Kowalik, P.J., Zaradny, H., 1978. Simulation of field water use and crop yield. In: Simulation Monographs, Pudoc, Wageningen.

Gärdenäs, A., Hopmans, J.W., Hanson, B.R., Šimůnek, J., 2005. Two-dimensional modeling of nitrate leaching for different fertigation strategies under micro-irrigation. Agric. Water Manage. 74, 219–242.

Grosse, W., Wissing, F., Perfler, R., Wu, Z., Chang, J., Lei, Z., 1999. Biotechnological approach to water quality improvement in tropical and subtropical areas for reuse and rehabilitation of aquatic ecosystems. Final report, INCO-DC Project Contract No. ERBIC18CT960059. Cologne, Germany.

Hansen, S., Jensen, H.E., Nielsen, N.E., Svendsen, H., 1990. DAISY: Soil Plant Atmosphere System Model. NPO Report No. A 10. The National Agency for Environmental Protection, Copenhagen, 272 pp.

Hanson, B.R., 1995. Practical potential irrigation efficiencies. In: Water Resources Engineering: Proceedings of the First International Conference. The American Society of Civil Engineers, San Antonio, TX, August 14–18.

Heinen, M., 2001. FUSSIM2: brief description of the simulation model and application to fertigation scenarios. Agronomie 21, 285–296.

Hopmans, J.W., Bristow, K.L., 2002. Current capabilities and future needs of rooot water and nutirent uptake modeling. Adv. Agron. 77, 104–175.

Hutson, J.L., Wagenet, R.J., 1991. Simulating nitrogen dynamics in soils using a deterministic model. Soil Use Manage. 7, 74–78.

Jansson, P.-E., Karlberg, L., 2001. Coupled Heat and Mass Transfer Model for Soil–Plant–Atmosphere systems. Royal Institute of Technology, Department of Civil and Environmental Engineering, Stockholm, 325 pp.

Kadlec, R.H., Knight, R.L., 1996. Treatment Wetlands. CRC Press, Boca Raton, FL, USA.

Ling, G., El-Kadi, A.I., 1998. A lumpbed parameter model for nitrogen transformation in the unsaturated zone. Water Resour. Res. 34 (2), 203–212.

Lotse, E.G., Jabro, J.D., Simmons, K.E., Baker, D.E., 1992. Simulation of nitrogen dynamics and leaching from arable soils. J. Contam. Hydrol. 10, 183–196.

May, D., Hanson, B., 2005. Effect of drip line placement on yield and quality of processing tomato (2004). Final report submitted to tomato processors.

Misra, C., Nielsen, D.R., Biggar, J.W., 1974. Nitrogen transformations in soil during leaching: I. Theoretical considerations. Soil Sci. Soc. Am. Proc. 38, 289–294.

Pierre, W.H., Banwart, W.L., 1973. Excess-base and excess-base/nitrogen ratio of various crop species and parts of plants. Agronomy J. 65, 91–96.

Selim, H.M., Iskandar, I.K., 1981. Modeling nitrogen transport and transformations in soils: 2. Validation. Soil Sci. 131, 303–312.

Silberbush, M., Barber, S.A., 1983. Prediction of phosphorus and potassium uptake by soybeans with a mechanistic mathematical model. Soil Sci. Soc. Am. J. 47, 262–265.

Šimůnek, J., Šejna, M., Van Genuchten, M.Th., 1999. The HYDRUS-2D software package for simulating two-dimensonal movement of water, heat, and multiple solutes in variable saturated media. Version 2.0, IGWMC-TPS-53. International Ground Water Modeling Center, Colorado School of Mines, Golden, Colorado.

Somma, F., Clausnitzer, V., Hopmans, J.W., 1998. Modeling of transient three-dimensional soil water and solute transport with root growth and water and nutrient uptake. Plant Soil 202, 281–293.

Tanji, K.K., Mehran, M., Gupta, S.K., 1981. Water and nitrogen fluxes in the root zone of irrigated maize. In: Frissel, M.J., van Veen, J.A. (Eds.), Simulation of Nitrogen Behavior of Sol–Plant Systems. PUDOC, Wageningen, the Netherlands, pp. 51–67.

Tillotson, W.R., Robbins, C.W., Wagenet, R.J., Hanks, R.J., 1980. Soil Water, Solute and Plant Growth Simulation, Bulletin 502. Utah Agricultural Experiment Station, 53 pp.

van Dam, J.C., Huygen, J., Wesseling, J.G., Feddes, R.A., Kabat, P., van Valsum, P.E.V., Groenendijk, P., van Diepen, C.A., 1997. Theory of SWAP, Version 2.0. Simulation of water flow, solute transport and plant growth in the Soil- Water-Atmosphere- Plant environment. Department of Water Resources, WAU, Report 71, DLO Winand Staring Centre, Wageningen, Technical Document 45.

van Genuchten, M.Th., 1980. A closed-form equation for predicting the hydraulic conductivity of unsaturated soils. Soil Sci. Soc. Am. J. 44, 892–1037.

Vrugt, J.A., Hopmans, J.W., Šimůnek, J., 2001. Calibration of a two-dimensional root water uptake. Soil Sci. Soc. Am. J. 65, 1027–1037.

Wagenet, R.J., Biggar, J.W., Nielsen, D.R., 1977. Tracing the transformation of urea fertilizer during leaching. Soil Sci. Soc. Am. J 41, 896–902.

Weinbaum, S.A., Johnson, R.S., Dejong, T.M., 1992. Causes and consequences of overfertilization in orchards. Proceedings of the Workshop Fertilizer Management in Horticultural Crops: Implications for Water Pollution, Hort. Technol. 2, 112–120.